

# ATTRIBUTES OF DIRECT MEASUREMENT OF INDUCTANCE IN A LOOP DETECTOR FOR TRAFFIC CONTROL

By:

S. Datta

J. Carroll

V. Petit

B. Sathyamangalam

R. Hebner

M. Grady

PR - 359

Center for Electromechanics  
The University of Texas at Austin  
PRC, Mail Code R7000  
Austin, TX 78712  
(512) 471-4496

# Simulation and Field Verification of Vehicle-Loop Interactions

Vincent Petit, Balaji Sathyamangalam, Robert Hebner, Fellow, IEEE, and Mack Grady, Fellow, IEEE  
*The University of Texas at Austin*

## ABSTRACT

Inductive sensors are used worldwide for traffic control. These sensors consist of a loop or loops of wire embedded in the pavement. The loops are connected to electronic control circuits that convert changes in loop inductance to signals to control traffic lights or to monitor traffic. This work describes a simulation approach that permits reliable calculation of the response of loops of various geometries to various types of vehicles. The simulation models both the loop and the vehicles with a set of filaments of finite length. The simulation approach was validated using two different loop geometries and various types of vehicles. The simulation was developed to assist in the selection of a loop geometry for a particular application or to assess the likely behavior of hypothetical loops. As it is based on a fundamental description of the vehicle-loop interaction, the simulation approach is also expected to be useful in other investigations of loop responses.

Index terms: inductive loop, simulation, splashover

## I. INTRODUCTION

The loop detector is a system used worldwide for traffic control. It generates a magnetic field and consists of a coil of wire buried into the pavement and energized by a current, typically in the frequency range between 10 and 20 kHz. When a vehicle passes over the loop, it passes through the magnetic field. Eddy currents are induced in the conducting portions of the vehicle and generate a magnetic field, which opposes the magnetic field of the loop, causing a decrease of the total magnetic field around the loop. Since the loop inductance is proportional to the magnetic flux, the loop inductance decreases.

In conventional operation, a loop detector unit is connected at the output of the loop. This is an oscillator whose resonant frequency depends upon the inductance of the loop. The change in resonant frequency due to the proximity of a vehicle is proportional to the inductance shift  $\Delta L/L$ . When the shift is above a preset threshold, the detector unit is actuated. This technology has spread throughout the world because it is reliable and relatively inexpensive.

There are significantly different reactions depending upon the type of vehicle that passes over the loop. A car will induce an inductance shift of roughly 5 to 6  $\mu\text{H}$  out of  $\sim 100 \mu\text{H}$  for the self-inductance of a square loop, while light vehicles or high-bed trucks may induce reactions as low as 0.1  $\mu\text{H}$ . To detect a light vehicle or a truck, the threshold must be set so that a 0.1  $\mu\text{H}$  inductance shift actuates the detector, according to NEMA Standards Publication, TS 1-1989, *Traffic Control Systems*. An important problem may arise from very low thresholds [1]. As the threshold is lowered, the detector becomes more sensitive to smaller perturbations of the magnetic field. Vehicles in the adjacent lanes of the road may induce a reaction large enough to mask the reactions of the light vehicles and high-bed trucks, thereby actuating the detector when low thresholds are set. This is called the “splashover” effect. Consequently, the operation of loops is the result of a tradeoff between detecting all vehicles and assuring immunity from the effects of vehicles in adjacent lanes.

It is generally both expensive and time-consuming to investigate alternative loop designs experimentally. To accelerate this work, a simulation package has been developed and verified that predicts loop-vehicle interaction at any spacing between the vehicle and loop. This investigation focuses on predictions of the loop response when the vehicle is passing either over the loop or on its adjacent lane. The loops considered were those whose designs are recorded in the "Traffic Detector Handbook" [2] plus two additional loop geometries to show that simulations may be useful in assessing alternative designs.

The approach in this investigation was to develop a simulation package, then to validate the simulations using a loop detector installed in a location in which we could record routine traffic flow of

an uncontrolled set of vehicles. Alternatively, we had the option of isolating that section of roadway to study particular interactions in more detail. The simulation approach and experimental verification are summarized in section II. The simulation package was then used to assess some effects of splashover. To do this, 18 loop geometries were evaluated for three vehicle types. The results of this simulation, which are summarized in the section III, led to the development of ratings for loop geometries for detection sensitivity, immunity to splashover, and discrimination. Finally, as described in Section IV, the simulation package was used to help determine some of the operational characteristics of a hypothetical new loop geometry.

## II. SIMULATION APPROACH

### A. Model Principles

The model is, at its core, a finite filament approach to the calculation of inductance [3]. The objects modeled are approximated by straight finite-length filaments. The integration is done from the centers of the filaments and the mutual inductance is calculated. A subroutine in MATLAB<sup>®</sup> was developed to compute the coupling between two pieces of wire. This subroutine calculates the inductance of a series of straight finite-thickness filaments. The calculation method performs a summation of the Neumann integrals of all the filaments. The integration is done from the centers of the filaments for the mutual inductance using a conventional approach [3].

This function in MATLAB<sup>®</sup> is the starting point of our simulations. The next step is to calculate the variation of inductance of the loop when the vehicle passes over or near it. The inductive coupling between the vehicle and the loop is calculated at different positions of the vehicle, which is equivalent to the variation of the coupling in time. From that variation of the coupling we find the variation of apparent inductance.

The inductive loop detector is a coil of wire whose geometry defines the finite filament size and orientation. The vehicle is more complicated to describe, since it is not a piece of wire, but is made of

conducting plates (the body of the vehicle) and a volume of metal (the engine). As developed in reference [2], a conducting plate may be approximated to a conducting mesh and then to a shorted turn of wire (Fig. 1), so the body of the vehicle is straightforward to model. The engine, by contrast, has a more complex geometry and can make a significant contribution to the vehicle-loop interaction. The volume of metal is represented as a number of adjacent conducting plates; we can model it using straight wire segments (Fig. 2). The model for the vehicle is eventually made of many coils of wire, all of which influence the loop coil. The program computes the mutual inductance between each coil of wire and the loop coil. The equivalent variation of inductance in the loop coil is shown in Fig. 3.

Computing the mutual inductance  $M$  for each coil of the vehicle, we get the variation of inductance  $-M^2/L_2$ . We add those variations and get the total variation of inductance of the inductive loop due to the vehicle. Then we compute the variation of inductance at several positions of the vehicles, simulating the vehicle travel as the vehicle passes over or near the loop or in the adjacent lane.

### *B. Vehicles – Basic Model*

Three vehicle models were developed and validated: a car, a motorcycle and a truck. The basic modeling approach goes beyond representing the vehicle as a single loop [4]. It is based on geometric measurements of the vehicles. The initial vehicle designs corresponded to real vehicles in terms of geometry. The basic and final models are shown in Figs. 4, 5, and 6, along with representations of the vehicles.

Although the initial vehicle models resembled the vehicles they represented, experiments showed they produced calculated results that differed significantly from the measured values. Experimental results are summarized in Table 1.

Thus, even though the models previously described complied with the geometry of the vehicles, they did not account adequately for the metallic parts of the vehicles or for the way eddy currents travel

through the vehicle. For example, the bottom of the car is far more complex than just a single conducting plate. Therefore, the model required considerable refinement.

### *C. Refined Model*

The new models have been compared with and refined using experimental data. The experiments were performed using a commercially available square test loop and diamond test loop provided by the Texas Department of Transportation. The vehicle models are validated using two different loops to ensure that the model can be used to predict the behavior of other shapes efficiently. The final vehicle models are shown in Figs. 4, 5, and 6.

### *D. Comparison of Theory with Experiment*

To validate the simulations, data were taken using a square loop and a diamond loop. The LABView<sup>®</sup>-based detector system measured loop voltage and current and calculated the impedance. The sampling interval used was about 0.05 s. The inductance was calculated at each sample and compared with the previous value. If the change was lower than a preset threshold, the process continued. If the change was greater than the given threshold, the detection was actuated and the transit of the vehicle was recorded.

Figs. 7 through 15 show the agreement between experimental results and simulation using the refined models. In each figure, the theoretical curve is represented by a dashed line, the experimental by a solid line. For some of the experimental data, the response is so small that digitization effects are visible. No measurements for the truck over the edge of the diamond loop were made, because reaction produced by a truck in an adjacent lane is within the range of precision of the acquisition system (i.e., a reaction of less than 0.1  $\mu\text{H}$ ) and is therefore irrelevant.

As shown in Table 2, the precision of the simulation is within the observed variations among vehicles within a class or for the same vehicle with small variations in the relative position with respect to the loop [5]. For the vehicles sensed at the road site used, the measured variation was 18% for the

trucks, 10% for cars and 7% for motorcycles. The models, therefore, report results within the range of the variation of the experimental data.

### **III. EFFECTS OF LOOP GEOMETRY**

#### *A. Simulation Results*

Using this simulation approach, we modeled 18 different loops that represent most of the shapes currently in use, plus two novel loop shapes. Any travel path in the vicinity loop may be simulated. To demonstrate the capability of the approach, this work focuses on two of the more significant paths. One is the vehicle passing directly over the loop, and the other is the vehicle passing the loop in lane adjacent to the lane in which the loop is located. For each loop shape, five different curves were calculated, representing the reaction of the car passing over the loop and on the adjacent lane of the loop, the motorcycle passing over the loop, the truck passing over the loop and on the adjacent lane of the loop. Because a motorcycle in the adjacent lane produces such a small effect, those data are ignored. The loop geometries that were examined are shown in Appendix 1.

Conventional detector electronics use the magnitude of the reaction to actuate the detector. So, although the simulation package produces interesting results on the shapes of the reactions, attention is given to the magnitude of the reactions to relate the results to the broad-base of field experience.

The purpose of this demonstration of the simulation package is to compare responses of different loop shapes. We identified six patterns of interest: the quality of the detection for each vehicle (car, motorcycle, truck) and the quality of the splashover mitigation for each vehicle (car, motorcycle, truck). The quality of those patterns varies, depending on the loop geometry. The purpose of the computations described here is to evaluate various loop geometries for different applications. For comparison, each loop is assigned a relative grade based on the results of the simulations for the conditions simulated. Since the square loop is the most common loop in use, the computations have been scaled so that loop

geometry always receives a score of 10. The computation equations are presented in Appendix 2 and tables that represent the rankings of the loops for each pattern appear in Appendix 3.

### *B. Assessment of Performance Characteristics*

The following interpretations are based on the tables described earlier and detailed in Appendix 3.

*D-Loop* As an example, the D-Loop used for motorcycle detection yields an excellent splashover immunity when detecting light vehicles; it yields a grade of 194.7 compared to 10 for the square loop (Table A-5). This means it is well suited for motorcycle detection, even though its grade in motorcycle detection is 5.5 compared to 10 for the square loop (Table A-2). The D-Loop does not yield a very strong reaction for motorcycles but, because of the high immunity to splashover effects, reliable decisions can be made even with the somewhat smaller direct responses.

*Rectangle* The rectangle is the best loop shape to use for truck detection with a grade of 25.1 (Table A-1). This is consistent with the general perception that as the size of the loop approaches the size of the vehicle, the better the detection. The rectangle matches the size of a truck better than the other loop geometries considered.

*Quadrupole* The quadrupole is designed to be installed at intersections as a presence detector. Since it is generally installed in cities, a great concern is light vehicle detection. All presence detections are large loops, to accommodate many vehicles over them. The quadrupole is the best large loop for motorcycle detection, as it has a grade of 2.1, compared to 1.4 for Rectangle and 0.6 for Rectangle 2 (Table A-2) and it is a very good loop for splashover immunity with a grade of 57.1 (Table A-5) when evaluated for motorcycle detection.

*Diamond* Use of the diamond loop is useful in cities, since it is one of the best loops for light vehicle detection with a grade of 17.6 (Table A-1) and also 10.3 on the general detection table (Table A-

3). The diamond grades are higher in both cases than those of the square loop (Tables A-2 and A-3). It also ranks among the best for splashover mitigation with a grade of 30.1 for trucks (Table A-4), 111.6 for motorcycles (Table A-5), and 111.6 in general (Tables A-1 and A-6).

Butterfly Tie Although the butterfly tie is a complex shape to create, it yields good results on the splashover mitigation, ranking among the first four loops in any splashover mitigation table (Tables A-4, A-5, and A-6). Indeed, it gets 102 in general splashover mitigation with 102 over the motorcycle records and 35.7 over the truck records. The butterfly tie does not give very good results in terms of quality of detection, but the threshold level for detection can be set low, since the splashover mitigation is very good.

Circle For detection, the circle scores 7.6 for trucks, 12.3 for motorcycles, and 10.2 in general. For splashover mitigation, it scores 32 for trucks, 51.8 for motorcycles and 51.8 in general (Appendix 3). These rankings are lower than those of the diamond loop. If circular, octagonal or hexagonal loops are being considered with the expectation of improved pavement life, these data provide information that might be useful in helping to compare the value of sensitivity being sacrificed with the value of the expected extension of service life.

### *C. Discrimination among Vehicles*

Over the past few years, studies [6, 7] have been conducted on the possible discrimination among vehicle types or even among individual vehicles by examining the magnitude of the reactions of the loops. To explore how useful this simulation would be in discrimination studies, a study of the discrimination among vehicle types for the loop shapes in appendix 1 was conducted using the simulation package. As expected, some loop shapes exhibit more discrimination capability than others by enhancing the difference in magnitude among the different vehicles. The results are detailed in Appendix 4. The best loop shape for discrimination purposes is the rectangle with a score of 18. The square loop comes fourth in the ranking.

## IV. TOWARD NEW SYSTEMS

To show that the simulation is useful in evaluating hypothetical loops, a new loop has been investigated. This new loop is composed of three rectangular multiturn loops, diagramed as loops 17 and 18 in Appendix 1. The short side of each rectangle is in the direction of travel, while the long side spans much of the width of the travel lane. This loop shows reasonable characteristics for sensitivity and immunity to splashover (Appendix 3). An interesting attribute is that the inductance variation as a vehicle passes over the loop is a multi-peaked curve, with the vehicle length being the primary contributor to the number of peaks. Specifically, as shown in Figs. 16-20:

- A car passing over the loop induces a two-peaked curve.
- A motorcycle passing over the loop induces a 3 peak-curve.
- A truck passing over the loop induces a 1 peak-curve.
- All the vehicles in splashover configuration induce a 1 peak-curve, which cannot be confused with the truck passing over the loop because of the different magnitude of the reaction.

This loop would have to be used with a new type of detector unit that would record the curve and/or count the number of peaks. No rigorous analysis has been performed using this hypothetical loop to estimate the change in response shape due to changes in vehicle speed [8]. Since the response is primarily due to the relative sizes of the individual loops and the vehicles, however, it is expected that if the detector has sufficient bandwidth, the response should be reasonably insensitive to speed. Similarly, if the distance between vehicles is more than a small fraction of the vehicle length, there should be little difficulty in separating closely spaced vehicles.

## V. CONCLUSIONS

The inductive loop detector is a rugged and inexpensive technology. It also yields good results, although some problems arise when trying to detect light or high-bed vehicles. Indeed, such vehicles

may have such a low reaction that vehicles in adjacent lanes induce a reaction of similar magnitude in the metered lane. This problem is called splashover. The practical approach to reducing the effects of splashover is to set a threshold level for detection so that the splashover signal is too small to be detected [2]. A simulation package was devised that permits the traffic engineer to assess, prior to cutting pavement and installing an inductive loop, how a specific loop geometry will react to both in-lane and adjacent-lane traffic. Knowing the size of the signals to be detected, as well as the size of the splashover signals, provides additional information as to the types of vehicles that will be detected reliably.

A simulation approach for vehicle-loop interactions was used. Simulation results were validated by installing a test loop and recording both routine traffic flows and staged tests for comparison purposes. The responses of 18 different loop shapes for both in-lane and adjacent-lane traffic of cars, trucks and motorcycles were predicted. From these results, relative responses of various loop geometries to a set of specified conditions were computed. These results suggest the simulation package can be used to extract information about loops currently in use and to help choose a particular shape, depending on some of the specific conditions of the application. Finally, it was shown the simulation package can be useful in assessing the likely performance of hypothetical loop designs. This work showed that key issues, such as splashover mitigation or discrimination among vehicles, are conveniently addressed within the model.

### **ACKNOWLEDGEMENT**

The authors wish to thank J. Kajs, who provided an initial version of a Matlab<sup>®</sup> subroutine for the inductance calculations.

### **REFERENCES**

1. R. A. Hamm and D. L. Woods, "Loop Detectors: Results of Controlled Field Studies," *ITE Journal*, pp. 12-16, November, 1992.
2. Traffic Detector Handbook, Institute of Transportation Engineers, Washington, D.C. 1997.

3. F. W. Grover, Inductance Calculations: Working Formulas and Tables, Dover Publications, Inc., 1946.
4. P. Russell and J. Smith, "Loop Detector Sensitivity Due to Burial Depth," Report FHWA-AZ87-826 to the Arizona Department of Transportation, 1987. (Available through NTIS as PB92167246.)
5. W. Guizhu C. Zonfa, and X. Langan, "Induction loop detection of bicycles flow based on pattern recognition (PR) techniques," *Trans. Sys. Theory and Appl. of Adv. Tech.*, Vol. 1, pp. 31-36, 1995.
6. J. Palen, et al, "California partners for advanced transit and highways (PATH) enhanced loop-based traffic surveillance program," *ITS Quarterly*, pp. 17-25, Fall, 2000.
7. C. Sun and S. Ritchie, "Heuristic vehicle classification using inductive signatures on freeways," *Transportation Research Record*, No. 1717, National Research Council, pp. 130-136, 2000.
8. C. Sun and S. Ritchie, "Individual vehicle speed estimation using single loop inductive waveforms," *J. Transportation Eng.*, Vol. 125, no. 6, pp. 531-538, 1999.

(footnote)

Manuscript submitted

V. Petit and B. Sathyamangalam were graduate students and M. Grady is a professor in the Electrical and Computer Engineering Department. R. Hebner is the Director of the Center for Electromechanics and a research professor in Mechanical Engineering.

This work was supported in part by the Texas Department of Transportation.

Table 1. Precision of the model using basic vehicle geometry

Vehicle	% difference between measured and calculated response
Car	50%
Motorcycle	83%
Truck	85%

Table 2. Precision of the model

Vehicle	% difference between measured and calculated response
Car	7.5%
Motorcycle	5.7%
Truck	9.0%

Fig. 1. Approximation of a conducting plate by a wire loop [2]

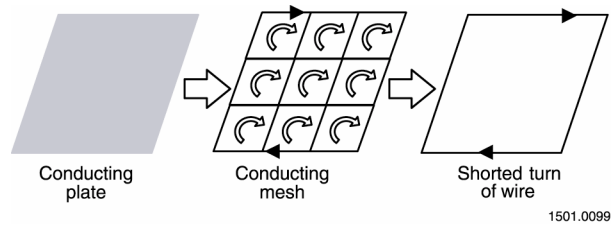
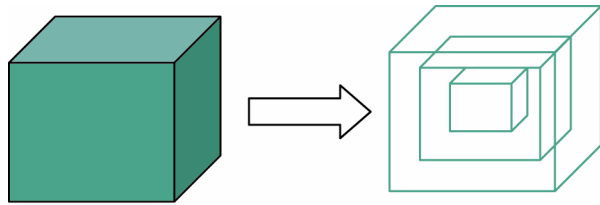
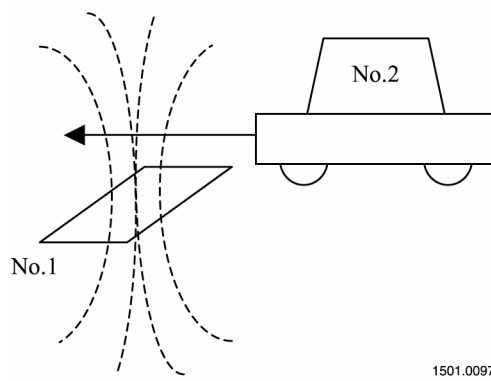


Fig. 2. Approximation of a motor by a set of loops



1501.0096

Fig. 3. Vehicle-loop interaction



1501.0097

$$\Phi(1 \rightarrow 2) = L_1 * i_1 + M * i_2$$

$$\Phi(2 \rightarrow 1) = 0 = L_2 * i_2 + M * i_1$$

$$\Rightarrow i_2 = -\frac{M}{L_2} * i_1$$

$$\Phi(1 \rightarrow 2) = (L_1 - \frac{M^2}{L_2}) * i_1 = L_{\text{apparent}} * i_1$$

Fig. 4. Basic model for the car, image of a car, and refined car model

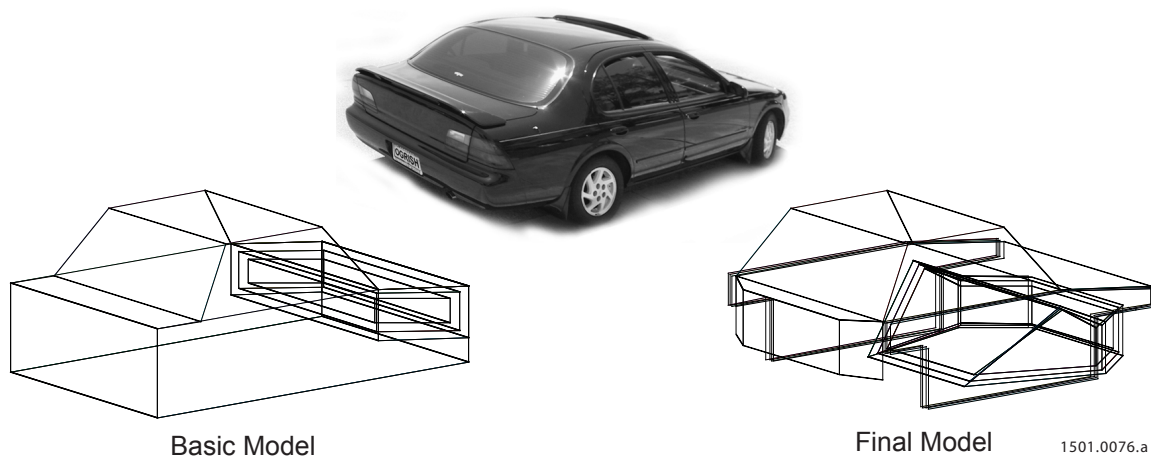


Fig. 5. Basic model for the truck, image of a truck, and refined truck model

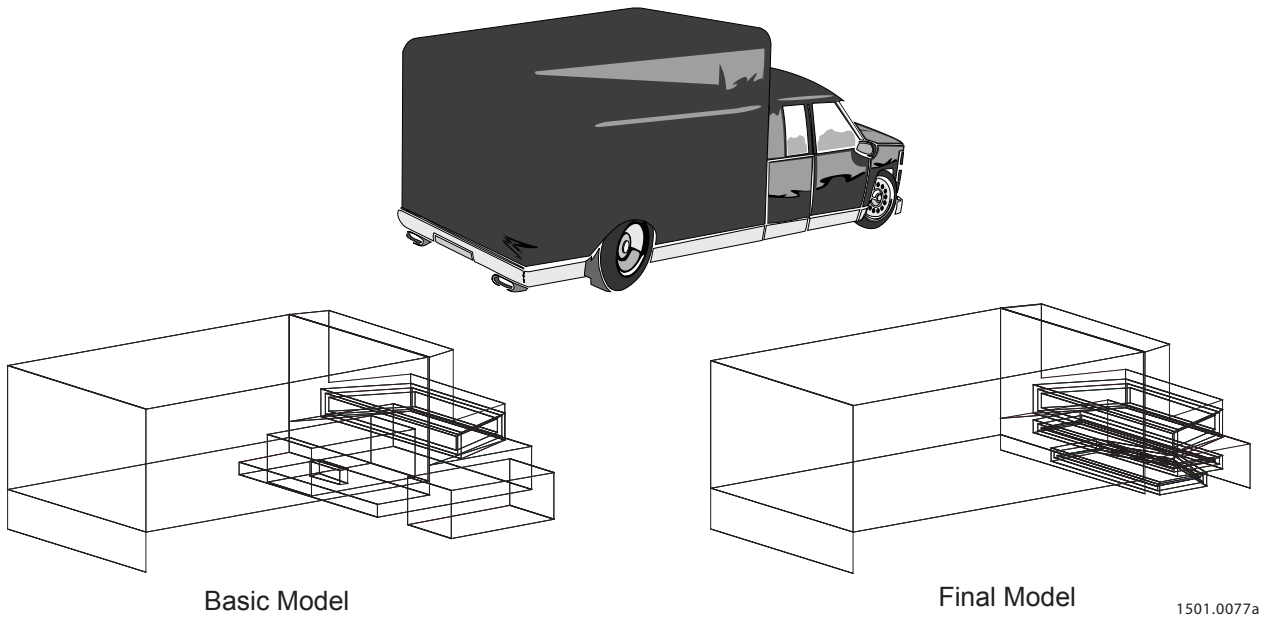


Fig. 6. Basic model for the motorcycle, image of motorcycle, and refined motorcycle model

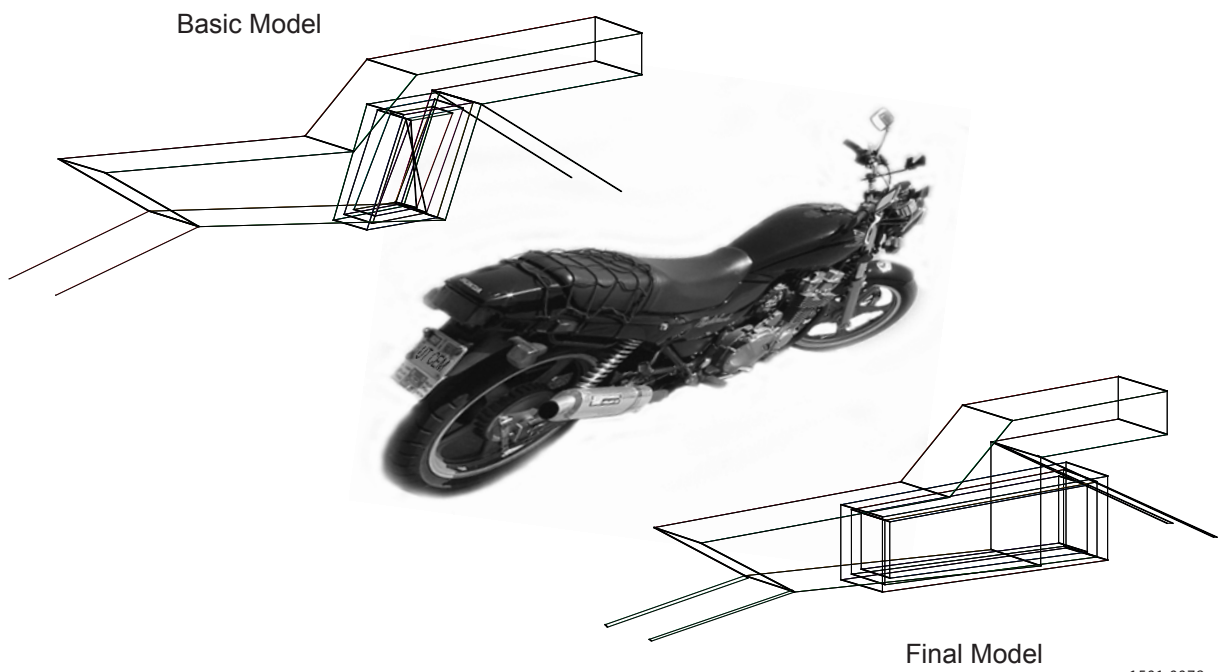


Fig. 7. Car passing over the square loop

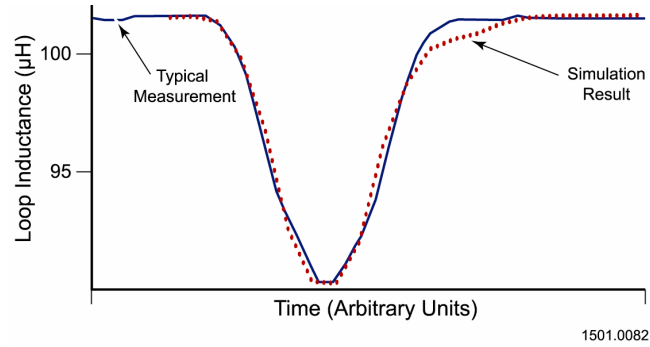


Fig. 8. Car on the edge of the square loop

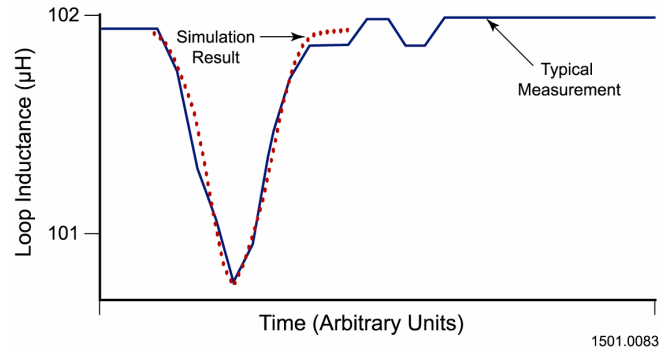


Fig. 9. Car passing over the diamond loop

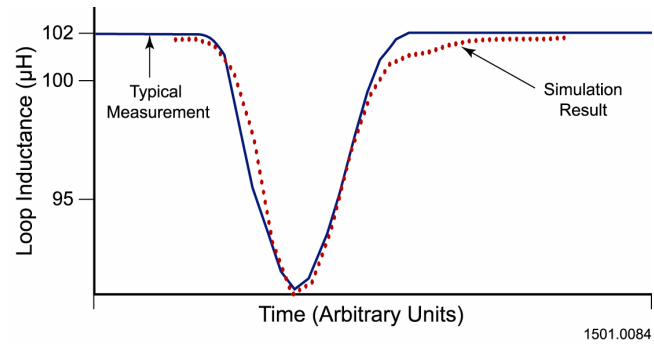


Fig. 10. Car on the edge of the diamond loop

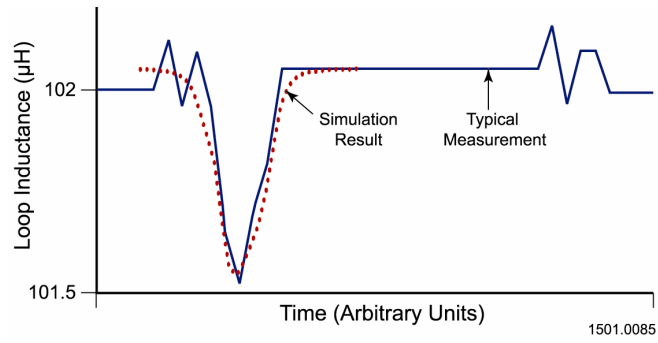


Fig. 11. Motorcycle passing over the square loop

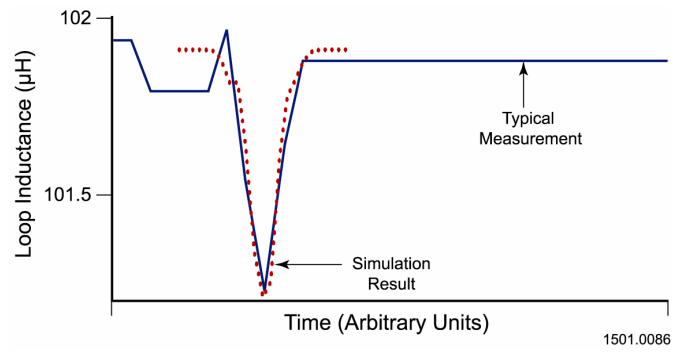


Fig. 12. Motorcycle passing over the diamond loop

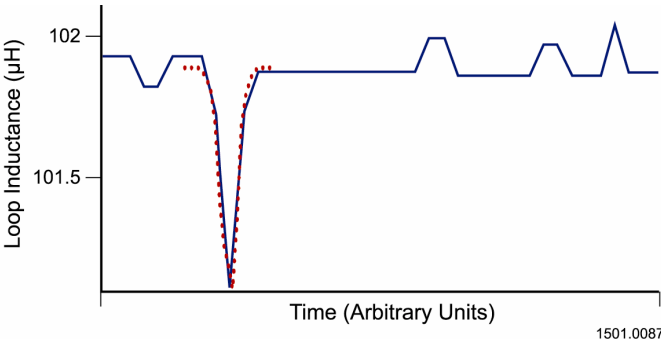


Fig. 13. Truck passing over the square loop

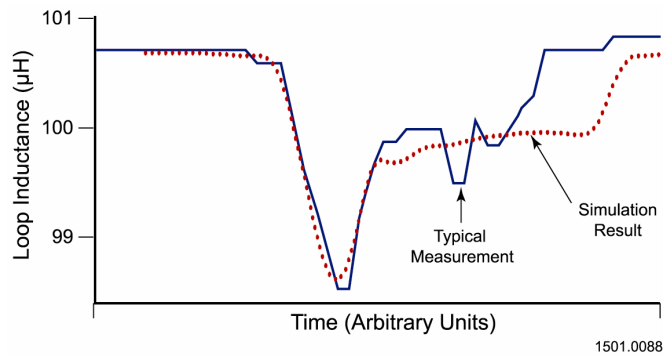


Fig. 14. Truck on the edge of the square loop

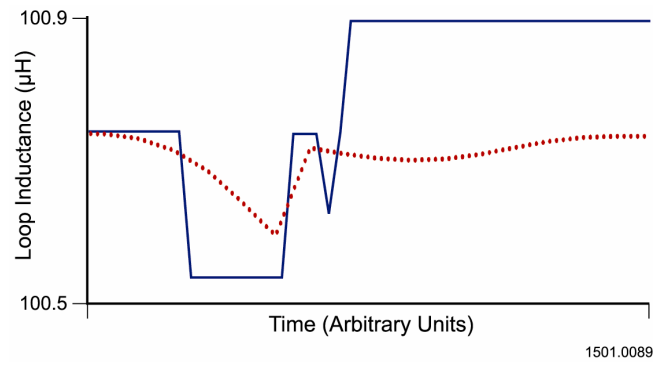


Fig. 15. Truck passing over the diamond loop

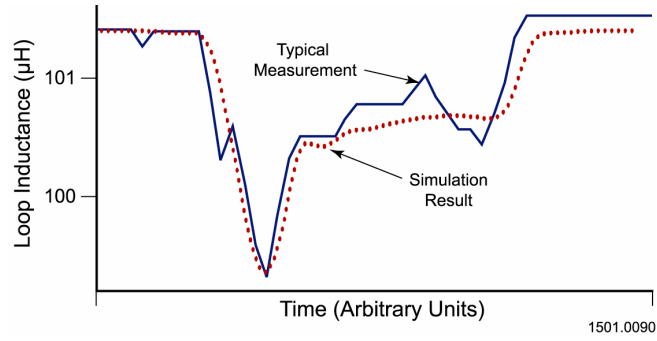


Fig. 16. Car passing over multiturn loop 2

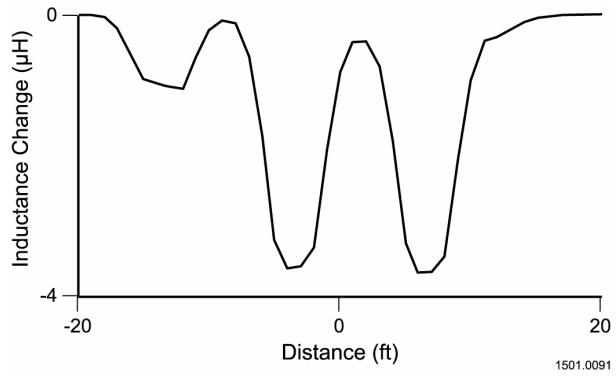


Fig. 17. Car passing on the adjacent lane of multiturn loop 2

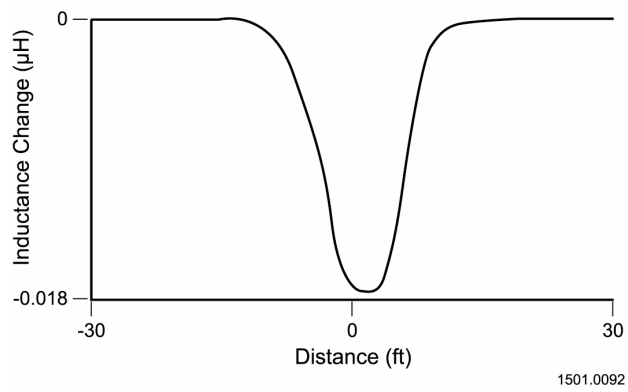


Fig. 18. Motorcycle passing over multiturn loop 2

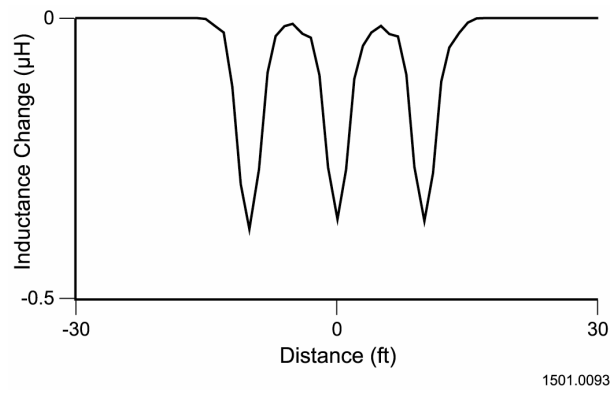


Fig. 19. Truck passing over multiturn loop 2

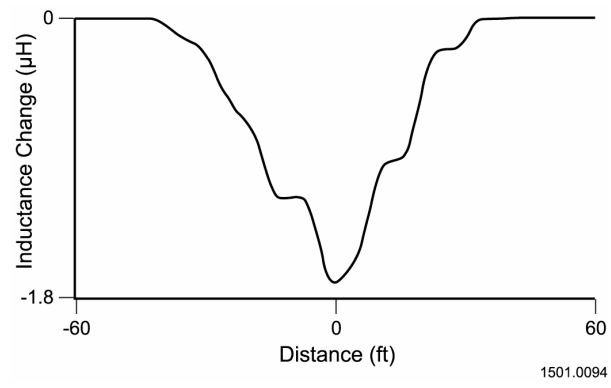
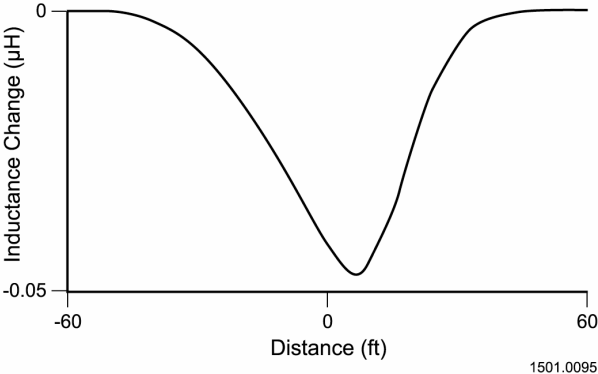
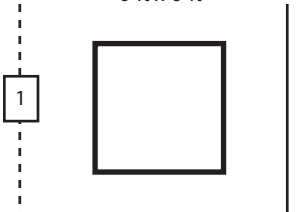
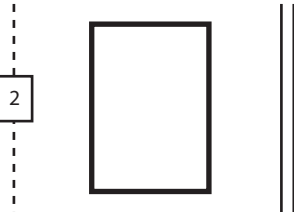
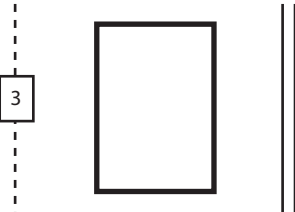
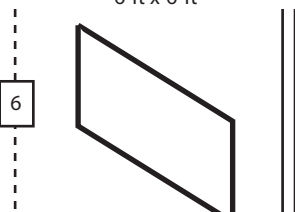
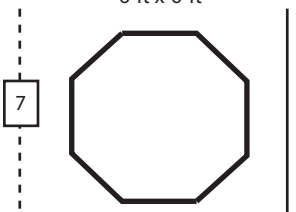
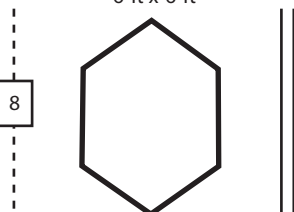
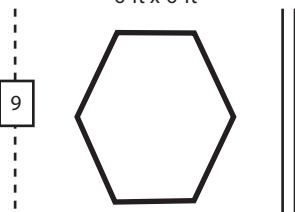
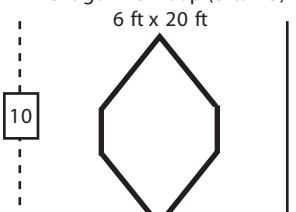
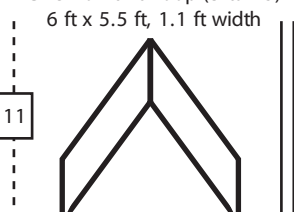
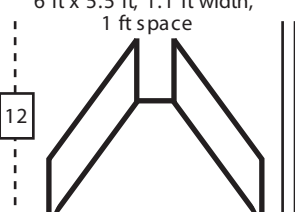
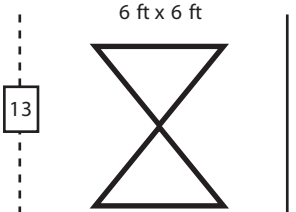
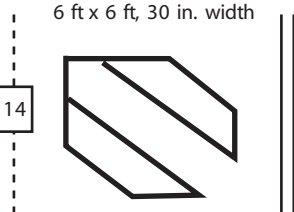
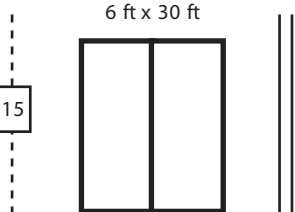
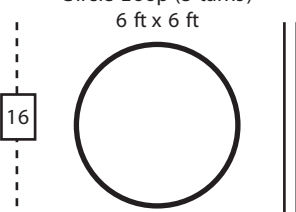
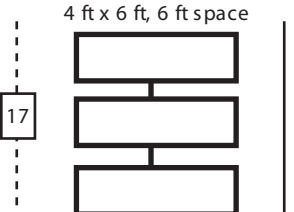
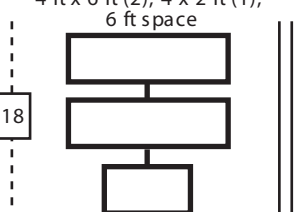


Fig. 20. Truck passing on the adjacent lane of horizontal



# APPENDIX 1

## LOOP SHAPES USED IN STUDY

<p style="text-align: center;">Square Loop (3 turns) 6 ft x 6 ft</p> <p style="text-align: center;">1</p> 	<p style="text-align: center;">Rectangle Loop (3 turns) 6 ft x 40 ft</p> <p style="text-align: center;">2</p> 	<p style="text-align: center;">Rectangle Loop (1 turn) 6 ft x 80 ft</p> <p style="text-align: center;">3</p> 
<p style="text-align: center;">Diamond Loop (3 turns) 6 ft x 6 ft</p> <p style="text-align: center;">4</p> 	<p style="text-align: center;">Triangle Loop (3 turns) 6 ft x 6 ft</p> <p style="text-align: center;">5</p> 	<p style="text-align: center;">Parallelogram Loop (3 turns) 6 ft x 6 ft</p> <p style="text-align: center;">6</p> 
<p style="text-align: center;">Octagon Loop (3 turns) 6 ft x 6 ft</p> <p style="text-align: center;">7</p> 	<p style="text-align: center;">Hexagon #1 Loop (3 turns) 6 ft x 6 ft</p> <p style="text-align: center;">8</p> 	<p style="text-align: center;">Hexagon #2 Loop (3 turns) 6 ft x 6 ft</p> <p style="text-align: center;">9</p> 
<p style="text-align: center;">Hexagon #3 Loop (3 turns) 6 ft x 20 ft</p> <p style="text-align: center;">10</p> 	<p style="text-align: center;">Chevron 0-ft Loop (3 turns) 6 ft x 5.5 ft, 1.1 ft width</p> <p style="text-align: center;">11</p> 	<p style="text-align: center;">Chevron 1-ft Loop (3 turns) 6 ft x 5.5 ft, 1.1 ft width, 1 ft space</p> <p style="text-align: center;">12</p> 
<p style="text-align: center;">Butterfly Loop (3 turns) 6 ft x 6 ft</p> <p style="text-align: center;">13</p> 	<p style="text-align: center;">Trapezoid Loop (3 turns) 6 ft x 6 ft, 30 in. width</p> <p style="text-align: center;">14</p> 	<p style="text-align: center;">Quadripole Loop (2-4-2 turns) 6 ft x 30 ft</p> <p style="text-align: center;">15</p> 
<p style="text-align: center;">Circle Loop (3 turns) 6 ft x 6 ft</p> <p style="text-align: center;">16</p> 	<p style="text-align: center;">Multiturn Loop #1 (3-3 turns) 4 ft x 6 ft, 6 ft space</p> <p style="text-align: center;">17</p> 	<p style="text-align: center;">Multiturn Loop #2 (3-3 turns) 4 ft x 6 ft (2), 4 x 2 ft (1), 6 ft space</p> <p style="text-align: center;">18</p> 

## APPENDIX 2

### EQUATIONS USED TO COMPUTE THE QUALITY OF VEHICLE DETECTION AND SPLASHOVER MITIGATION

Variables:

- $V_C$  = value of a car
- $V_T$  = value of a truck
- $V_M$  = value of a motorcycle
- $V_W$  = worst value
- (*SL*) = for/with the square loop
- (*AL*) = on an adjacent lane

Quality of the detection ( $Q_d$ ):

$$Q_d(\text{truck}) = V_T \times \frac{10}{V_T(\text{SL})}$$

$$Q_d(\text{motorcycle}) = V_M \times \frac{10}{V_M(\text{SL})}$$

$$Q_d(\text{general}) = \frac{V_C \times \frac{10}{V_C(\text{SL})} + (1) + (2)}{3}$$

Quality of the splashover mitigation ( $Q_{sm}$ ):

$$Q_{sm}(\text{truck}) = V_W \left( \frac{V_T}{V_C(\text{AL})}; \frac{V_T}{V_T(\text{AL})} \right) \times \frac{10}{V_W \left( \frac{V_T}{V_C(\text{AL})}(\text{SL}); \frac{V_T}{V_T(\text{AL})}(\text{SL}) \right)}$$

$$Q_{sm}(\text{motorcycle}) = V_W \left( \frac{V_M}{V_C(\text{AL})}; \frac{V_M}{V_T(\text{AL})} \right) \times \frac{10}{V_W \left( \frac{V_M}{V_C(\text{AL})}(\text{SL}); \frac{V_M}{V_T(\text{AL})}(\text{SL}) \right)}$$

$$Q_{sm}(\text{general}) = V_W \left( \frac{V_M}{V_C(\text{AL})}; \frac{V_M}{V_T(\text{AL})}; \frac{V_T}{V_C(\text{AL})}; \frac{V_T}{V_T(\text{AL})} \right) \times \frac{10}{V_W \left( \frac{V_M}{V_C(\text{AL})}(\text{SL}); \frac{V_M}{V_T(\text{AL})}(\text{SL}); \frac{V_T}{V_C(\text{AL})}(\text{SL}); \frac{V_T}{V_T(\text{AL})}(\text{SL}) \right)}$$

## APPENDIX 3 - DETECTION AND SPLASHOVER RESULTS

Tables A-1 through A-6 can be used to choose among several loops the one that best matches a given combination of patterns of interest. They provide a good understanding of the strengths and weaknesses of each loop shape.

Table A-1. Detection (trucks)

Loop	Grade
1 Rectangle	25.1
2 Hexagon 3	12.0
3 Rectangle 2	11.0
4 Square	10.0
5 Octagon	8.4
6 Circle	7.6
7 Hexagon 2	7.1
8 Hexagon	6.8
9 Multiturn Loop 1	5.4
10 Diamond	4.8
11 Multiturn Loop 2	4.1
12 Parallelogram	3.6
13 Triangle	3.4
14 Butterfly tie	2.8
15 Chevron 0 ft	0.4
16 Chevron 1 ft	0.3
17 D Loop	0.2
18 Quadrupole	0.008

Table A-2. Detection (motorcycles)

Loop	Grade
1 Diamond	17.6
2 Hexagon 2	15.7
3 Hexagon	14.9
4 Octagon	13.7
5 Circle	12.3
6 Parallelogram	11.9
7 Triangle	11.5
8 Square	10.0
9 Butterfly tie	8.3
10 Hexagon 3	6.7
11 Multiturn Loop 2	6.3
12 D loop	5.5
13 Multiturn Loop 1	4.6
14 Chevron 0 ft	2.5
15 Quadrupole	2.3
16 Rectangle	1.4
17 Rectangle 2	0.6
18 Chevron 1 ft	0.3

Table A-3. Detection (general)

Loop	Grade
1 Hexagon 2	11.7
2 Octagon	11.4
3 Hexagon	10.5
4 Diamond	10.3
5 Circle	10.2
6 Square	10.0
7 Rectangle	9.5
8 Hexagon 3	8.6
9 Parallelogram	6.4
10 Triangle	6.2
11 Butterfly tie	5.3
12 Multiturn loop 2	4.4
13 Rectangle 2	4.2
14 Multiturn loop 1	4.1
15 D Loop	2.1
16 Chevron 0 ft	1.1
17 Quadrupole	0.7
18 Chevron 1 ft	0.3

Table A-4. Splashover (trucks)

Loop	Grade
1 Hexagon	194.7
2 Butterfly Tie	35.7
3 Circle	32.0
4 Hexagon	31.6
5 Diamond	30.1
6 Parallelogram	25.0
7 Multiturn loop 2	24.8
8 Chevron 1 ft	23.7
9 Hexagon 3	20.6
10 Multiturn Lop 1	19.6
11 Chevron 0 ft	17.2
12 Rectangle	15.6
13 Octagon	12.9
14 Square	10.0
15 D Loop	8.3
16 Triangle	7.1
17 Rectangle 2	2.4
18 Quadrupole	0.2

Table A-5. Splashover (motorcycles)

Loop	Grade
1 D Loop	194.7
2 Diamond	111.6
3 Chevron 0 ft	111.4
4 Butterfly Tie	102.0
5 Hexagon 2	83.5
6 Parallelogram	82.6
7 Hexagon	69.7
8 Quadrupole	56.4
9 Circle	51.8
10 Multiturn Loop 2	38.2
11 Chevron 1 ft	25.2
12 Triangle	23.4
13 Octagon	21.3
14 Multiturn Loop 1	16.4
15 Hexagon 3	11.5
16 Square	10.0
17 Rectangle	0.8
18 Rectangle 2	0.1

Table A-6. Splashover (general)

Loop	Grade
1 Diamond	111.6
2 Chevron 0 ft	111.4
3 Butterfly Tie	102.0
4 Hexagon 2	83.5
5 Parallelogram	82.6
6 Hexagon	69.8
7 D Loop	65.8
8 Circle	51.8
9 Multiturn Loop 2	38.2
10 Chevron 1 ft	25.2
11 Triangle	23.4
12 Octagon	21.3
13 Multiturn Loop 1	16.4
14 Hexagon 3	11.5
15 Square	10.0
16 Quadrupole	1.7
17 Rectangle	0.8
18 Rectangle 2	0.1

## APPENDIX 4

### EQUATION USED TO COMPUTE DISCRIMINATION AMONG VEHICLES

Variables:

- $D$  = discrimination
- $V_C$  = value of a car
- $V_T$  = value of a truck
- $V_M$  = value of a motorcycle
- $(SL)$  = for/with the square loop

Equation :

$$D = (V_C - V_M) \times \left( \frac{10}{(V_C - V_M)(SL) + 10 * (V_C - V_T)} \right) \times \left( \frac{10}{(V_C - V_T)(SL) + 10 * (V_T - V_M)} \right) \times \left( \frac{V_T(SL) - V_M(SL)}{21} \right)$$

Corresponding Table:

Table A-7. Discrimination

	Loop	Grade
1	Rectangle	10.8
2	Octagon	10.8
3	Hexagon 2	10.6
4	Square	10.0
5	Circle	9.7
6	Hexagon	8.6
7	Hexagon 3	8.5
8	Rectangle 2	8.0
9	Diamond	6.9
10	Butterfly Tie	4.0
11	Parallelogram	3.2
12	Multiturn Loop 1	3.2
13	Multiturn Loop 2	3.2
14	Triangle	3.1
15	D Loop	0.7
16	Chevron 0 ft	0.3
17	Chevron 1 ft	0.3
18	Quadrupole	0.2